TRABALHO COMPUTACIONAL DE CALC. NUMÉRICO

GRUPOS 1 e 2

1) Resolver o sistema de equações não-lineares para $0 \leq \alpha \leq 360°$:

$$g_1 = x_0 \sin\alpha - y_0 \cos\alpha = 0 \qquad (1)$$

$$g_2 = (y_{c_1} - y_0)(y_{c_2} - y_0) + (x_{c_1} - x_0)(x_{c_2} - x_0) = 0 \qquad (2)$$

$$g_3 = \frac{x_1^2}{a^2} + \frac{y_1^2}{b^2} - 1 = 0 \qquad (3)$$

$$g_4 = (x_1 - x_{c_1})^2 + (y_1 - y_{c_1})^2 - r^2 = 0 \qquad (4)$$

$$g_5 = \frac{x_2^2}{a^2} + \frac{y_2^2}{b^2} - 1 = 0 \qquad (5)$$

$$g_6 = (x_2 - x_{c_2})^2 + (y_2 - y_{c_2})^2 - r^2 = 0 \qquad (6)$$

$$g_7 = x_0^2 + y_0^2 - d^2 = 0 \qquad (7)$$

$$g_8 = y_1\left[x_1\left(\frac{b^2}{a^2} - 1\right) + x_{c_1}\right] - y_{c_1} x_1 \frac{b^2}{a^2} = 0 \qquad (8)$$

$$g_9 = (x_{c_1} - x_0)^2 + (y_{c_1} - y_0)^2 - (y_{c_2} - y_0)^2 - (x_{c_2} - x_0)^2 = 0 \qquad (9)$$

$$g_{10} = y_2\left[x_2\left(\frac{b^2}{a^2} - 1\right) + x_{c_2}\right] - y_{c_2} x_2 \frac{b^2}{a^2} = 0 \qquad (10)$$

onde, para $\underset{\sim}{g}(\underset{\sim}{u}) = 0$, tem-se:

$$\underset{\sim}{u} = (x_0, y_0, x_{c_1}, y_{c_1}, x_{c_2}, y_{c_2}, x_1, y_1, x_2, y_2)$$

— 1 —

2) Como valor inicial p/ a solução iterativa, use a solução aproximada de $\alpha = 90°$, com o algoritmo abaixo:

```
if (a.le.b) then
   y1 = a/sqrt(2.dØ)
else
   dum = (a*a-((d-r*sqrt(2.))/sqrt(2.))**2)/
         ((a/b)**2-1.)
   if (dum.le.Ø.) then
      y1=0.
      else
      y1 = sqrt(dum)
   endif
endif
x1 = a*sqrt(1.-y1*y1*(1./b)**2)
xc1 = x1 + r/sqrt(2.)
yc1 = y1 + r/sqrt(2.)
x0 = 0.
y0 = d
x2 = -x1
y2 = y1
xc2 = -xc1
yc2 = yc1
```

3) Recomenda-se o uso da linguagem FORTRAN. Além disso, recursos do diretório "Numerical Recipes" do FORTRAN 90 instalados nos computadores do LENA-3 podem ser utilizados.

4) Apresentar saídas gráficas do comportamento de $\underset{\sim}{u} \times \alpha$, isto é, $(x_0 \times \alpha;\ y_0 \times \alpha;\ x_1 \times \alpha \ldots)$

5) Cada grupo deverá apresentar um disquete com o seu programa e um relatório na forma de artigo Técnico p/a. serem entregues até o último dia de aula do semestre

6) Cada grupo deverá resolver o sistema utilizando um método diferente:

GRUPO 1: NEWTON-RAPHSON
GRUPO 2: NEWTON-RAPHSON MODIFICADO

OBS: ESTE PROBLEMA REFERE-SE AO CÁLCULO DA POSIÇÃO DOS PONTOS MARCADOS NA FIGURA DO MECANISMO DE CILINDRÓIDES EM ANEXO, EM FUNÇÃO DO ÂNGULO α.

VALORES DOS PARÂMETROS GEOMÉTRICOS:

$a = 8,5$
$d = 11,1$
$r = 1,3$
$b = 6,5 = b_1 = b_2$

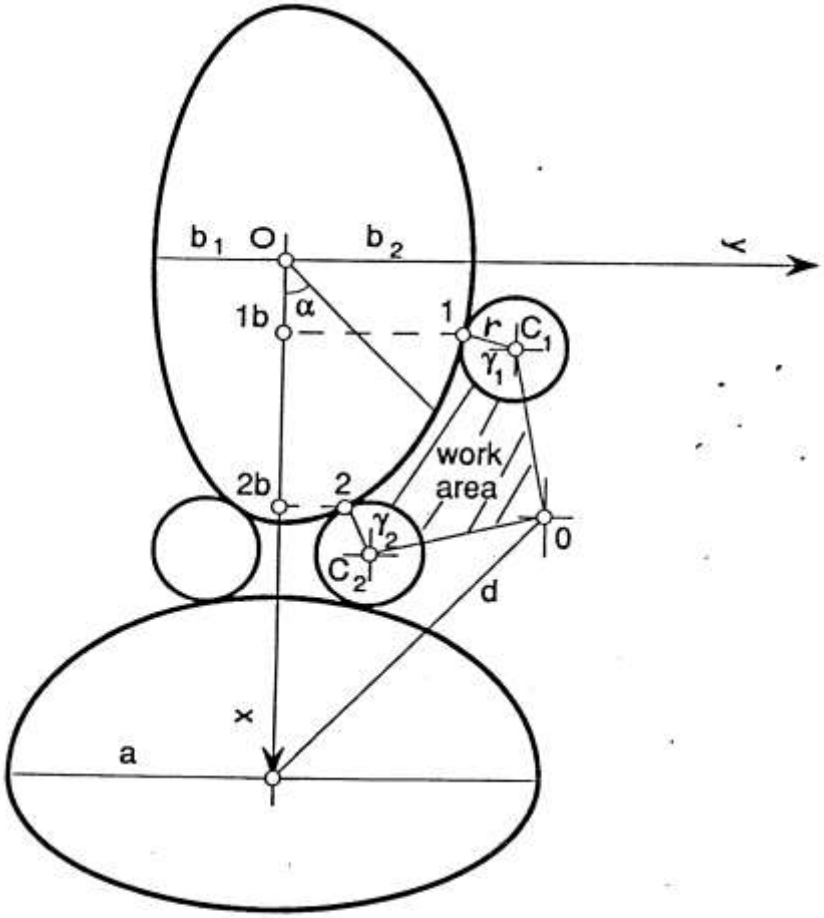

Figure - The geometrical parameters. The work area. The local coordinates system.

ICE-Vol. 22, Heavy Duty Engines: A Look at the Future
ASME 1994

ANALYSIS OF A CYLINDROIDS ROTARY ENGINE

José V. C. Vargas and Razvan Florea
Department of Mechanical Engineering and Materials Science
Duke University
Durham, North Carolina

ABSTRACT

In this paper a kinematic and thermodynamic analysis of a new engine based on a rotating cylindroids mechanism is presented. A comparison between the performances of the piston engine and the novel engine, both operating in the Otto cycle with the same compression ratio, is given. A higher expansion ratio than the compression ratio is obtained by the use of asymmetrical ellipses. The expansion stroke is extended, increasing the work production without adding additional energy in the combustion process. Based on a theoretical analysis, the new mechanism is shown to have a significant gain in thermal efficiency in comparison with the piston engine. For the new mechanism, the condition of minimum required work can be achieved easier and for a larger range of equivalence ratio than for the crank-piston mechanism.

INTRODUCTION

The history of internal combustion engines had its start in the mid-nineteenth century. Since then, most of the research efforts have been dedicated to the engine operating with the well known crank-piston mechanism. Hence, much research has been done to increase efficiency and specific power, dealing with problems such as avoidance of combustion knock, combustion-chamber design, emissions, mixture preparation and spark timing. In addition to that, the relatively recent introduction of electronics into the engine systems has brought the state of the art in crank-piston engines to a high level of development. In parallel to the crank-piston history, new development directions were considered. For example, rotary engines have been proposed. Among them, the most famous is the Wankel engine, which received considerable research attention from several corporations and scientists as reported by Norbye (1971), who also presents a survey on other rotary engines.

Much has been done on alternative fuels research, as for coal-fueled diesel engines (McMillian, 1989) and in the development of multifuel engines, such as the works of Hardenberg (1982) and Duggal (1984). The combustion process has been a constant subject of research and how it affects the search for increasing efficiency (Thomas, 1979). Also, mechanical design improvement has been sought by the increase in the number of valves and, eventually, valve event optimization to improve the cam design (Assanis, 1989). The works of Rychter (1985) and Abenavolli (1991) suggest mechanical modifications in the conventional crank-piston mechanism to provide a variable compression ratio which allows the engine to operate at the maximum possible compression ratio, for any load and speed, thus increasing the efficiency. In the conventional design, the compression ratio is fixed and determined by the critical detonation condition, given by the high load and low speed operation regime.

The advanced stage of evolution of the piston engine obviously implies that a change in the mechanism

should be acceptable only if a real gain in efficiency and specific power is possible to be achieved. As a result, the necessary investment in the research and implementation of a new design would be a justifiable effort.

The objective of this study is to present a new rotary mechanism, designed by Mello (1990), that can be applied to internal combustion engines and to show that a significant gain in efficiency can be achieved in comparison with a piston engine, operating at the same compression ratio. The new mechanism consists on the rotation of four cylindroids with asymmetric ellipses sections, separated by eight rolling sealing cylinders, kept together through springs. As a result, a working volume is created in the middle of the cylindroids. The main advantage of the new mechanism is that a higher expansion ratio than the compression ratio is possible to be obtained without any increase in the total size of the engine. The expansion stroke is extended, increasing the work production without adding additional energy in the combustion process. This feature would make possible the use of a low octane number fuel in a spark ignition engine, such as kerosene, since low compression ratios could be used, this way avoiding detonation. Also, the advantages of all other rotary mechanisms in comparison with the crank-piston mechanism are herein present, such as: ports could be used, instead of valves, for admission and exhaust; reduction of the number of parts; high power to weight ratio and high volumetric efficiency. In comparison with the Wankel engine, it should be noted that the new engine does not show any eccentricities.

THEORY

In this section, a kinematic and thermodynamic analysis for the new mechanism is presented. Hence, kinematic and thermodynamic constraints are identified for the new design, and a performance comparison between the crank-piston engine and the new engine is made possible too, both operating in a four-stroke cycle. The new mechanism requires only one revolution of the crankshaft for each power stroke.

Kinematic Analysis

The new mechanism can be described with the help of Fig. 1. It is shown schematically in the position of minimum volume. Four cylindroids(1) with asymmetric ellipses sections spin towards the same direction, around the respective axes(2), keeping a convenient distance between their surfaces, in a way that eight rolling sealing cylinders(3) are kept together through springs(4). The working volume(5) varies with the movement of the cylindroids. The whole mechanism can be protected by a box(6) for assembling, cooling and lubrication purposes. The idea is to transmit the rotating movement through four planetary gears connected to the axes of the cylindroids, and then to a solar gear connected to a main central axis. The admission and the exhaust processes could be undertaken without valves, through channels in the cylindroids axes communicating with appropriately dimensioned ports, located on the lateral surfaces of the cylindroids.

Fig. 2 shows a sequence of positions of the new mechanism corresponding to the processes of the Otto cycle shown in Fig. 3: admission (0-1), compression (1-2), combustion (2-3), expansion (3-4) and exhaust (4-0).

The volume variation with respect to the rotation angle α of the new mechanism can be obtained by the definition of a local coordinates system with its origin located on the center of the cylindroid, and noting the geometric symmetries of the design, as shown in Fig. 4.

For a set of parameters a, b_1, b_2, d, r, a nonlinear system of equations can be constructed with respect to the local coordinates system, where a and b are the ellipses parameters, with indices 1 and 2 referring to each asymmetrical half of the ellipses, d is the distance between the center of the mechanism and the center of the ellipses and r is the radius of the circles. The unknowns are chosen to be the coordinates (x, y) of five characteristic points: the center of the mechanism, the two centers of the circles and the two tangential points between the circles and the ellipses.

Based on the geometry of Fig. 4, the equations can be written for any angle position α, as follows:

$$g_1 = x_0 sin\alpha - y_0 cos\alpha = 0 \quad (1)$$

$$g_2 = (y_{C_1} - y_0) \cdot (y_{C_2} - y_0) + (x_{C_1} - x_0) \cdot (x_{C_2} - x_0) = 0 \quad (2)$$

$$g_3 = \frac{x_1^2}{a^2} + \frac{y_1^2}{b^2} - 1 = 0 \quad (3)$$

$$g_4 = (x_1 - x_{C_1})^2 + (y_1 - y_{C_1})^2 - r^2 = 0 \quad (4)$$

$$g_5 = \frac{x_2^2}{a^2} + \frac{y_2^2}{b^2} - 1 = 0 \quad (5)$$

$$g_6 = (x_2 - x_{C_2})^2 + (y_2 - y_{C_2})^2 - r^2 = 0 \quad (6)$$

$$g_7 = x_0^2 + y_0^2 - d^2 = 0 \quad (7)$$

$$g_8 = y_1 \left[x_1 \left(\frac{b^2}{a^2} - 1 \right) + x_{C_1} \right] - y_{C_1} x_1 \frac{b^2}{a^2} = 0 \quad (8)$$

$$g_9 = (x_{C_1} - x_0)^2 + (y_{C_1} - y_0)^2 -$$

$$(y_{C_2} - y_0)^2 - (x_{C_2} - x_0)^2 = 0 \qquad (9)$$

$$g_{10} = y_2\left[x_2\left(\frac{b^2}{a^2} - 1\right) + x_{C_2}\right] - y_{C_2}x_2\frac{b^2}{a^2} = 0 \qquad (10)$$

where in equations (3), (5), (8) and (10), if circles "1" or "2" are on the half ellipse "1", $b = b_1$, otherwise $b = b_2$.

The nonlinear system

$$g_i(x_0, y_0, x_{C_1}, y_{C_1}, x_{C_2}, y_{C_2}, x_1, y_1, x_2, y_2; \alpha) = 0, \quad i = 1, \ldots, 10$$

can be solved numerically for each angle α using a Newton-Raphson scheme.

Once the solution is obtained, the volume at each position α can be calculated using the following expression:

$$V_d(\alpha) = 4h[S_{\Delta OC_1C_2} + S_{\square C_1 12C_2} + S_{\square 11_b2_b2} - S_{\frown 11_b2_b2} - S_{\angle\gamma_1} - S_{\angle\gamma_2}] \qquad (11)$$

where S is the surface area defined by each index, h is the height of the cylindroids and the quantity between brackets is the work area shown in Fig. 4.

Kinematic constraints have to be imposed such that the mechanism can operate: a solution of the system of equations (1) to (10) can exist for any α; the circles do not intersect and the distance between ellipses should be always less than $2r$ and greater than 0.

Thermodynamic Analysis

In this section, in order for comparing the performances of the new mechanism and the traditional crank-piston, two ideal analyses are given. One based on the air cycle and the other on the fuel-air cycle.

Many detailed models describing the behaviour of an internal combustion engine, flow and heat transfer processes in it, such as the works of O'Rourke (1987), Amsden et al. (1985) and Schock et al. (1984) have been published. For simplicity, just the ideal analyses are herein presented, in order to identify the qualitative trends of the new rotary engine, in comparison with the piston engine.

Fig. 3 shows schematically the constant volume cycle where the processes of admission (0-1), compression (1-2), combustion (2-3), expansion (3-4) and exhaust (4-0) can be identified.

The engine is treated as a closed system in both analyses in the discussion that follows.

Air Cycle. The air cycle for the piston engine is defined by points 1 - 2 - 3 - 4'- 1 in Fig. 3. The assumptions for the air cycle can be summarized as uniform properties throughout the control volume, isentropic compression (1-2), heat absorption at constant volume (2-3), isentropic expansion (3-4') and heat rejection at constant volume (4'-1). The air cycle for the rotary engine is defined by points 1 - 2 - 3 - 4 - 5 - 1 in Fig. 3. With the new mechanism, the exhaust process (4-1) is idealized in two stages: heat rejection at constant volume (4-5), followed by a combination of heat rejection and work at constant pressure (5-1). It is assumed constant specific heat at constant volume (c_v) and constant specific heat at constant pressure (c_p) in all processes and dry air as an ideal gas. The new mechanism offers the venue for extra expansion because the expansion volume (3-4) is bigger than the compression volume (1-2), different from the piston engine, where the compression and expansion volumes are equal.

For the crank-piston mechanism, as it is well known, the thermal efficiency is given by:

$$\eta_P(r_1) = 1 - \frac{1}{r_1^{k-1}} \qquad (12)$$

where $r_1 = \frac{V_1}{V_2}$ and $k = \frac{c_p}{c_v}$.

For the new mechanism, it can be written:

$$\eta_R = \frac{W_{net}}{Q_{input}} = \frac{(U_4 - U_3) - (U_2 - U_1) - p_{d1}(V_{d5} - V_{d1})}{U_3 - U_2} \qquad (13)$$

where W_{net} is the resulting work from the thermodynamic cycle, Q_{input} is the heat input due to the combustion process, U is the internal energy, p_d is the dimensional pressure and the numerical indices refer to the Otto cycle presented in Fig. 3.

Or, in terms of temperature and volume ratios:

$$\eta_R(r_1, r_2, \tau) = 1 - \frac{1}{r_1^{k-1}} \cdot \frac{\tau \cdot r_2^{k-1} - 1 + (k-1)\cdot\left(\frac{1}{r_2} - 1\right)}{\tau - 1} \qquad (14)$$

where $\tau = \frac{T_3}{T_2}$, $r_2 = \frac{V_1}{V_3}$ and T is the dimensional temperature.

It must be noted that for $r_2 = 1$ the cylindroid is symmetric and $\eta_R = \eta_P$.

The question that arises from equation (14) is what would be the highest possible efficiency to be obtained from the new mechanism in comparison with a piston engine of known compression ratio r_1.

In order to gain maximum efficiency for a fixed r_1 and a known heat input (fixed τ), the numerator of the second term in the right hand side of equation (14) has to be minimized. The maximum efficiency is attained for $r_{2opt} = \frac{1}{\tau^{1/k}}$.

The optimal ratio coincides with a limit thermodynamic constraint. In Fig. 3, the hypothetical point H represents the intersection of the isentropic line of the expansion process and the atmospheric pressure level. Hence, point H determines the minimum r_2 which can exist, for producing work with the exhaust gases. The following sequence of equalities results from the assumptions of the problem:

$$\frac{1}{r_{2H}} = \frac{V_H}{V_1} = \frac{T_H}{T_1} = \frac{T_H}{T_3} \cdot \frac{T_3}{T_2} \cdot \frac{T_2}{T_1} = \tau \cdot r_{2H}^{k-1} \quad (15)$$

therefore

$$r_{2H} = \frac{1}{\tau^{1/k}} = r_{2opt} \quad (16)$$

From the above analysis, a restriction $1 \geq r_2 \geq r_{2H}$ arises. For a given compression ratio r_1, the maximum efficiency as a function of r_{2H}, setting $\tau = r_{2H}^k$ in equation (14), is obtained as:

$$\eta_{RH} = \eta_R(r_1, r_{2H}, \tau) = 1 - \frac{1}{r_1^{k-1}} \cdot \frac{\left(\frac{1}{r_{2H}} - 1\right) k}{\frac{1}{r_{2H}^k} - 1} \quad (17)$$

From equations (12) and (14), the gain in efficiency of the new mechanism with respect to the piston engine can be represented by the following quantity:

$$\frac{\eta_R - \eta_P}{\frac{1}{r_1^{k-1}}} = 1 - \frac{\tau \cdot r_2^{k-1} - 1 + (k-1) \cdot \left(\frac{1}{r_2} - 1\right)}{\tau - 1} \quad (18)$$

Equation (18) provides an insight on the possible efficiency gain $\forall r_1$, as a function of r_2 and τ.

For designing purposes, it is important to determine whether or not the engine will provide a minimum work as required by the project (W_{req}). Therefore, the condition $W_{net} \geq W_{req}$ has to be satisfied. From equation (13), it is possible to write:

$$W_{net} = \eta_R(U_3 - U_2) \quad (19)$$

Hence, the work condition will be satisfied if:

$$(\tau - 1) - \frac{\tau \cdot r_2^{k-1} - 1 + (k-1) \cdot \left(\frac{1}{r_2} - 1\right)}{r_1^{k-1}} \geq \frac{W_{req}}{mc_v T_2} \quad (20)$$

where m is the total mass of working fluid.

It should be noted that for a fixed compression ratio r_1, the temperature T_2 results. Therefore, the nondimensional group $\frac{W_{req}}{mc_v T_2}$ accounts for the required work expected for a given r_1.

Fuel-Air Cycle. In the fuel-air cycle, the engine is also treated as a closed system, with the same assumptions as the air cycle, except that: now the working fluid is a mixture of fuel, air and products assumed gaseous. The heat absorption process is a result of a combustion reaction started by an electric spark and the combustion process is considered in chemical equilibrium and at constant volume. The pressure during the admission and exhaust process is considered constant and equal to the atmospheric pressure. The specific heats of the fluid, both at constant pressure and constant volume, are considered variable as functions of temperature. In the compression process, combustion or chemical reaction is assumed not to occur. The fluid is a homogeneous mixture of ideal gases.

In order to compute the efficiency of the fuel-air cycle, the thermodynamic analysis must be performed in each process, determining the net work and the available heat of combustion.

The combustion process is assumed to happen for a fuel in the form $C_m H_n$, according to the following equation, as reported by Bejan (1988):

$$C_m H_n + \lambda \left(m + \frac{n}{4}\right) \cdot (O_2 + 3.76 N_2) \rightarrow a_1 CO_2 + a_2 H_2O + a_3 O_2 + a_4 CO + a_5 H_2 + a_6 N_2 \quad (21)$$

where λ is the equivalence ratio, defined as the actual air-fuel ratio divided by the stoichiometric air-fuel ratio.

The coefficients of the products in equation (21) depend on λ. For $\lambda > 1$, the reaction happens with excess air, and $a_1 = m$, $a_2 = \frac{n}{2}$, $a_3 = (\lambda - 1) \cdot \left(m + \frac{n}{4}\right)$, $a_4 = 0$, $a_5 = 0$ and $a_6 = 3.76\lambda \left(m + \frac{n}{4}\right)$. For $\lambda = 1$, the reaction happens with theoretical air, and the coefficients are the same as in the reaction with excess air, except that $a_3 = 0$. For $\lambda < 1$, the reaction develops with low air, and as it is well known, for low air, the mixture of products contains CO in addition to CO_2, H_2O and N_2, and, possibly other components. This composition will depend on the products' temperature and pressure. For simplicity, the analysis herein presented assumes the combustion happens as in equation (21), which will provide means to compare the performance of the two mechanisms operating with low air. The coefficients are then computed based on the assumption of the formation of H_2 according to an average mass fraction of 1.5% of the

products, as it can be deduced from products composition charts as the ones reported by De Hershey et al. (1936). The calculated coefficients for the low air reaction are then, $a_1 = 0.985\left[2.088\lambda\left(m+\frac{n}{4}\right)-\frac{n}{2}-m\right]$, $a_5 = a_1 + \frac{n}{2} + m - 2\lambda\left(m+\frac{n}{4}\right)$, $a_2 = \frac{n-2a_5}{2}$, $a_3 = 0$, $a_4 = 2\lambda\left(m+\frac{n}{4}\right) - 2a_1 - a_2$ and $a_6 = 3.76\lambda\left(m+\frac{n}{4}\right)$.

In the beginning of each cycle, a residual fraction of the products f, remains in the combustion chamber, while a new charge is admitted, thus the number of moles of unburned mixture per unit mass of air is given by:

$$n_{um} = n_p f + n_r(1-f) \tag{22}$$

where $n_p = \frac{n_{tp}}{n_{tair}w_{air}}$, $n_r = \frac{n_{tr}}{n_{tair}w_{air}}$, with n_{tp} and n_{tr} obtained from the coefficients of the appropriate reaction (low, theoretical or excess air), the indices p, r, tp, tr and $tair$ refer to products, reactants, total of products, total of reactants and total of air, respectively, and w is the molecular weight.

The fuel-air ratio is given by:

$$r_{fa} = \frac{w_{fuel}}{n_{tair}w_{air}} \tag{23}$$

The following nondimensional groups can be defined for temperature, pressure, volume and internal energy per unit mass of air:

$$\theta = \frac{T}{T_0} \tag{24}$$

$$p = \frac{p_d}{p_{d0}} \tag{25}$$

$$V = \frac{V_d}{V_{d1}} \tag{26}$$

$$u = \frac{u_d}{p_{d0}V_{d1}} \tag{27}$$

where T_0 and p_{d0} are, respectively, the ambient temperature and atmospheric pressure. Now, a reference volume is introduced to account for the variation of n_{um} with respect to λ:

$$V_{ref} = \frac{V_{dref}}{V_{d1}} = \frac{n_{um}\bar{R}_0T_0}{p_{d0}V_{d1}} \tag{28}$$

In the beginning of the compression process, it can be written:

$$\theta_1 = \frac{1}{V_{ref}} \tag{29}$$

Now, using the appropriate equation (low, theoretical or excess air) and the known internal energy of each reactant, given in tabular form as by Obert (1950), the internal energy of the mixture of gases is obtained by:

$$u = \frac{\sum_{i=1}^{reac,prod} x_i w_i u_i(\theta)}{\sum_{i=1}^{reac,prod} x_i w_i} \tag{30}$$

Likewise, c_p and c_v can be obtained by:

$$c = \frac{\sum_{i=1}^{reac,prod} x_i w_i c_i(\theta)}{\sum_{i=1}^{reac,prod} x_i w_i} \tag{31}$$

where c could represent c_p or c_v, the superscript of the sum $reac, prod$ could mean either number of reactants or number of products, which depend on the reaction type and the index i refers to each component of the mixture.

Isentropic compression and expansion are herein assumed, therefore taking into account that c_p and c_v are given functions of temperature such as reported by Obert (1950), k is computed for each volume position as:

$$k_j = \frac{c_{p_j}(\theta_j)}{c_{v_j}(\theta_j)} \tag{32}$$

where the index j refers to each volume position.

Hence, assuming piecewise constant k, pressure and temperature at each volume position can be obtained from:

$$p_j = p_{j-1}\left(\frac{V_{j-1}}{V_j}\right)^{k_{j-1}} \tag{33}$$

$$\theta_j = \theta_{j-1}\left(\frac{p_j}{p_{j-1}}\right)^{\frac{k_{j-1}-1}{k_{j-1}}} \tag{34}$$

In this fashion, p_2, θ_2, p_4 and θ_4 are obtained at the end of the compression and expansion processes.

The internal energy at state 2 is obtained as in equation (30) for a temperature θ_2.

The variation of internal energy due to the combustion process can be evaluated by computing the low heating value of the fuel at θ_2 (Van Wylen, 1965) as:

$$\begin{aligned}\bar{u}_c &= U_{prod} - U_{reac} \\ &= \sum_{i=1}^{prod} n_i\left[\bar{h}_f^0 - \bar{R}_0T_0 + \Delta\bar{u}\right]_i - \\ &= \sum_{i=1}^{reac} n_i\left[\bar{h}_f^0 - \bar{R}_0T_0 + \Delta\bar{u}\right]_i\end{aligned} \tag{35}$$

According to the definition of the nondimensional internal energy given by equation (27), taking into account the fuel-air ratio, that equation (35) expresses molal quantities, the residual fraction of products, and that $\bar{u}_c$ is a negative quantity, a nondimensional heat of combustion can be written as:

$$u_c = -\frac{\bar{u}_c}{w_{fuel}p_{d0}V_{d1}} \cdot r_{fa} \cdot (1-f) \tag{36}$$

For low air, the above equation neglects the heat of combustion due to CO and H_2 that are assumed present within the products, since the combustion is incomplete, and part of the available mass of fuel does not burn.

The internal energy in the beginning of the expansion process u_3 is obtained by adding up the available heat of combustion according to the reaction (low, theoretical or excess air).

Once u_3 is known, the temperature at state 3, θ_3, results from the known internal energy of each product as a function of temperature, the assumed reaction and equation (30).

Now, from the equation of state for ideal gases and the defined nondimensional groups, it can be written:

$$p_3 = \frac{n_p}{n_{um}} \cdot \frac{\theta_3}{V_3} \cdot V_{ref} \tag{37}$$

The internal energy at the end of the expansion process u_4 can be obtained through equation (30), since θ_4 is known from equation (34), and p_4 from equation (33), as well.

At the end of the expansion process, point 4, the exhaust valve opens and the combustion products remaining in the cylinder may be assumed to have undergone an adiabatic reversible expansion up to the atmospheric pressure (Obert, 1950). This hypothetical process determines an hypothetical volume as follows:

$$V_H = V_4 \left(\frac{p_5}{p_4}\right)^{\frac{k-1}{k}} \tag{38}$$

This volume represents the space the entire weight of working fluid would occupy, as a closed system according to the process described above. Hence, the residual fraction that remains in the combustion chamber on the exhaust stroke is given by:

$$f = \frac{V_0}{V_H} \tag{39}$$

The thermal efficiency of the fuel-air cycle can be computed either for the crank-piston mechanism or the rotary mechanism as:

$$\eta_P \text{ or } \eta_R = \frac{(u_3 - u_4) - (u_2 - u_1) - p_5(V_5 - V_1)}{u_c} \tag{40}$$

Note that, for the crank-piston mechanism, the last term in the numerator of equation (40) does not exist, since the expansion volume is equal to the compression volume.

Learning from the air cycle analysis, a nondimensional quantity $\frac{\eta_R - \eta_P}{1/r_1^{k-1}}$ can also be defined, in order to access the gain in efficiency of the new mechanism in comparison with the crank-piston mechanism, since a similar behaviour is expected in the fuel-air cycle. For that, k is assumed approximately constant and equal to k_{air}. The behaviour of the above defined nondimensional group is therefore expected to be nearly independent of r_1.

The same thermodynamic constraint $1 \geq r_2 \geq r_{2H}$, observed in the air cycle has to be satisfied here. Thus, V_H and r_{2H} are computed and for a fixed r_1, a limit is established through $\eta_{RH}(r_{2H}, \lambda)$.

A designing condition $W_{net} \geq W_{req}$ can be imposed, where W_{req} is a minimum required work. For a fixed r_1, $1 \geq r_2 \geq r_{2H}$, an appropriate value of λ_{crit} that satisfies the work condition can be determined. For low air, λ_{crit} is a minimum and for excess air, λ_{crit} is a maximum, therefore determinig a conditional efficiency limit that satisfies the work condition, for a fixed r_1. For comparison purposes, W_{req} could be specified as the work produced by the crank-piston engine ($r_2 = 1$) with a fixed ratio r_1, and theoretical air.

NUMERICAL APPROACH

For the kinematic analysis, an approximate solution for $\alpha = 90°$ is computed separately and the Newton method is used to track the actual solution of equations (1) to (10) at each particular angle α. Once the solution of the system is known, the volume can be computed for each angle α.

For the thermodynamic analysis, in order to compute the fuel-air cycle, the residual fraction f has to be determined. An iterative method based on an appropriate initial guess for f is used to obtain the correct residual fraction. A secant method is used in the fuel-air cycle, to solve for the appropriate λ that achieves the limit work condition $W_{net} = W_{req}$, for each r_2 and fixed r_1.

RESULTS AND DISCUSSION

In order to validate the model used for the fuel-air ideal analysis (no losses included), calculations were performed for the crank-piston mechanism ($r_2 = 1$) with different λ and r_1. The results show good agreement with experimental data for a real cycle as reported by Taylor (1985), mainly when $r_1 < 9$.

In order to evaluate the potential of the new mechanism for practical applications, calculations are performed for different geometrical and thermodynamical parameters. Assuming a characteristic unit length, all the geometrical parameters are therefore dimensionless. A given length $d = 11.1$ and a corresponding length $a = 8.5$ are assumed.

The question that arises is what pairs (r, b) will satisfy the geometrical conditions. In Fig. 5 the region that satisfies the kinematic constraints is shown.

To illustrate the volume variation of the working space, Fig. 6 shows $V_d(\alpha)$ for several possible combinations $(r, b_1/b_2)$, where it can be noticed the compression volume is smaller than the expansion volume. Also, for a fixed r, the volume gap increases as b_1/b_2 decreases. The kinematic condition is represented by the smallest possible ratio b_1/b_2. Points 0, 1, 2, 3, 4 and 5 corresponding to the Otto cycle are also shown.

In Figs. 7 and 8 the efficiency of the rotary engine η_R versus the volume ratio r_2 for the air and fuel-air cycles is represented. The compression ratio r_1 is fixed $(r_1 = 6)$. The combustion temperature ratio τ and the minimum required work W_{req} are used as parameters for the air cycle. The parameters for the fuel-air cycle are the equivalence ratio λ and W_{req}. For the air cycle, η_R does not depend on τ for large values of r_2 (close to 1) and increases when r_2 decreases. For the fuel-air cycle, η_R increases when r_2 decreases and the slopes of the curves η_R versus r_2 (for different λ) do not depend on λ. For the air cycle, for a variation in $r_2 = 1$ to 0.42 (kinematics constraints) the increase in η_R is about $\Delta\eta_R = 0.10$ to 0.12. Similarly, for the fuel-air cycle the increase in η_R is about $\Delta\eta_R = 0.08$ to 0.10. For the air cycle, imposing W_{req} as the work done by the crank-piston mechanism, from equation (20), a lower limit for the working region results. Similarly, for the fuel-air cycle, imposing W_{req} as the work done by the crank-piston mechanism (with theoretical air $\lambda = 1$), a closed working region results. In both air and fuel-air cycles the efficiency of the rotary engine is always greater than the efficiency of the crank-piston engine for the same required work.

In Fig. 9, for the fuel-air cycle, the efficiency of the rotary engine η_R versus r_1, for different r_2 as a parameter, is shown. The curves show a similar variation for both the rotary engine $(r_2 < 1)$ and the crank-piston engine $(r_2 = 1)$.

Equation (18) shows that, for the air cycle, the group $\frac{\eta_R - \eta_P}{1/r_1^{k-1}}$ does not depend on r_1. Fig. 10 shows a similar behaviour for the fuel-air cycle as well.

In Fig. 11, the same group $\frac{\eta_R - \eta_P}{1/r_1^{k-1}}$, is represented versus r_2 for both air cycle $(\tau = 5)$ and fuel-air cycle $(\lambda = 1)$. The theoretical air mixture $(\lambda = 1)$ shows a combustion temperature ratio $\tau = 5$ in the fuel-air simulation, thus this value is chosen for the reference air cycle, for comparison purposes. From the graphic, one could see that a simple analysis of the increase in efficiency for the air cycle is valid also for the fuel-air cycle and does not depend on r_1.

In Fig.12, the equivalence ratio λ versus volume ratio r_2 with $\frac{W_{req}}{p_{a0} V_{d1}}$ as parameters is represented. For a minimum required work (W_{req}), the equivalence ratio λ can vary in a large range defined by the lower limit $(\lambda < 1)$ and the upper limit $(\lambda > 1)$ with the new mechanism $(r_2 < 1)$, and still achieve the work condition. This feature gives a considerable advantage in comparison with the crank-piston mechanism.

CONCLUSIONS

The kinematic and thermodynamic analysis of a new engine based on a rotary cylindroids mechanism is presented. From the previous discussion, some very important features of the new mechanism can be emphasized.

1. As a result of the theoretical analysis herein presented, the new mechanism is shown to have a significant gain in efficiency in comparison with the piston engine, operating at the same compression ratio.

2. For the new mechanism, the condition of minimum required work can be achieved easier, at higher efficiency and for a larger range of equivalence ratio than for the crank-piston mechanism.

3. A higher expansion ratio than the compression ratio is obtained. The expansion stroke is extended, increasing the work production without adding additional energy in the combustion process. This feature would make possible the use of a low octane number fuel in a spark ignition engine, such as kerosene, since low compression ratios could be used, this way avoiding detonation.

The advantages of all other rotary mechanisms in comparison with the crank-piston mechanism are herein present, such as: ports could be used, instead of valves, for admission and exhaust; reduction of the number of parts; high ~~weight-power~~ power-to-weight ratio and high volumetric efficiency.

From the kinematic and thermodynamic analysis, the engine could be considered for a deeper analysis. Hence, a dynamic analysis including mass and heat loss, incomplete combustion and frictional losses, should be considered as a future work.

REFERENCES

Abenavoli, R. J., Sciaboni, A. and Wardzinsky, W., 1991, "Performance Analysis of a Variable Stroke reciprocating engine", *Proceedings of the 26th Intersociety Energy Conversion Engineering Conference - IECEC*, Boston, MA, Vol. 5, pp. 1-7.

Amsden, A. A., Ramshaw, J. D., O'Rourke, P. J. and Dukowicz, J. L., 1985, "KIVA: A Computer Program for Two and Three-Dimensional Fluid Flows with Chemical Reactors and Fuel Sprays", Los Alamos National Laboratory Report LA-10245-MS.

Assanis, D. N. and Polishack, M., 1989, "Valve Event Optimization in a Spark-Ignition Engine", *The Eleventh Annual Fall Technical Conference of the ASME Internal Combustion Engine Division*, The American Society of Mechanical Engineers, ICE - Vol.9, pp. 201-208.

Bejan, A., 1988, "Advanced Engineering Thermodynamics", Wiley, New York, NY, Chapter 7.

Duggal, V. K., Kuo, T. W. and Lux, F. B., 1984, "Review of Multifuel Engine Concepts and Numerical Modeling of In-Cylinder Flow Processes in Direct Injection Engines", SAE Paper 840005.

Hardenberg, H. O. and Buhl, H. W., 1982, "The Mercedes-Benz OM 403 VA - A Standard Production, Compression-Ignition, Direct-Injection Multifuel Engine", SAE Paper 820028.

Hershey, A. E., Eberhardt, J. E. and Hottel, H. C., 1936, "Thermodynamic Properties of the Working Fluid in Internal Combustion Engines", *SAE Journal*, Vol. 39, No. 4, p. 409.

McMillian, M. H. and Webb, H. A., 1989, "Coal-Fueled Diesels: Systems Development", *The Twelfth Annual Energy-Sources Technology Conference and Exhibition*, The American Society of Mechanical Engineers, ICE - Vol. 7, pp. 1-8.

Mello, M. L. M., 1990, Private Communication.

Norbye, J. P., 1971, "The Wankel Engine", Chilton Book Company.

Obert, E. F. and Jennings, B. H., 1950, "Internal Combustion Engine Analysis and Practice", International Textbook Company, Chicago, IL, Chapter 7.

O'Rourke, P. and Amsden, A., 1987, "Three Dimensional Numerical Simulation of the UPS-292 Stratified Charge Engine", SAE Paper 870597.

Rychter, T. J. and Teodorczyk, A., 1985, "VR/LE Engine with a Variable R/L during a single cycle", *SAE Annual Congress*, Detroit, MI, SAE Paper 850206.

Rychter, T. J. and Teodorczyk, A., 1985, "Economy and NO potential of a SI Variable R/L Engine", *SAE Annual Congress*, Detroit, MI, SAE Paper 850207.

Schock, H. J., Sosoka, D. J. and Ramos, J. I., 1984, "Formation and Destruction of Vortices in a Motored Four-Stroke Piston-Cylinder Configuration", *AIAA Journal*, Vol. 22, pp. 948-9.

Taylor, C. F., 1985, "The Internal-Combustion Engine in Theory and Practice", The M. I. T. Press, 2nd Edn, Vol. 1, Chapter 2, p. 36.

Thomas, A., 1979, "The Scope for Increasing the Efficiency of Automotive Engine through Combustion Research", University of Cambridge, Report CVED/A - Thermo/TR 10.

Van Wylen, G. J. and Sonntag, R. F., 1965, "Fundamentals of Classical Thermodynamics", Wiley, New York, NY, Chapter 12.

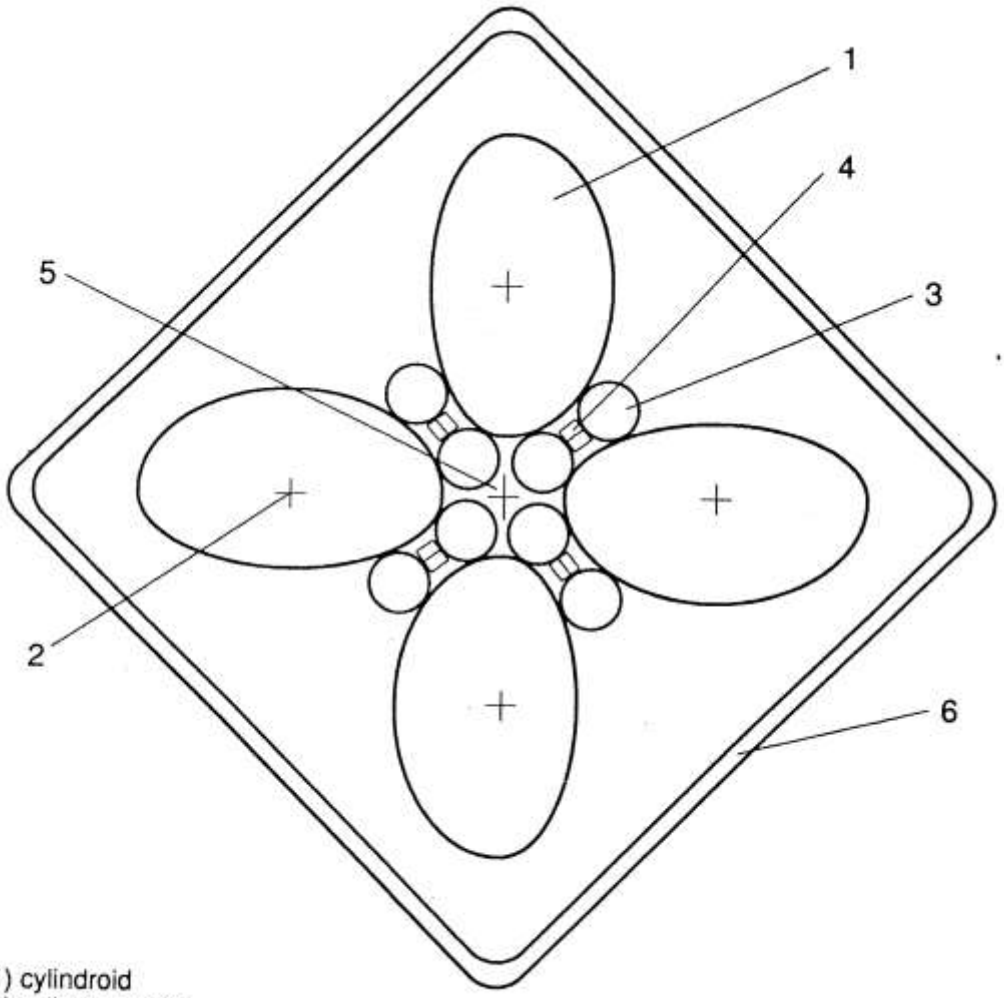

1) cylindroid
2) cylindroid axis
3) sealing cylinder
4) spring
5) working volume
6) assembling box

Figure 1 - Description of the new mechanism.

223

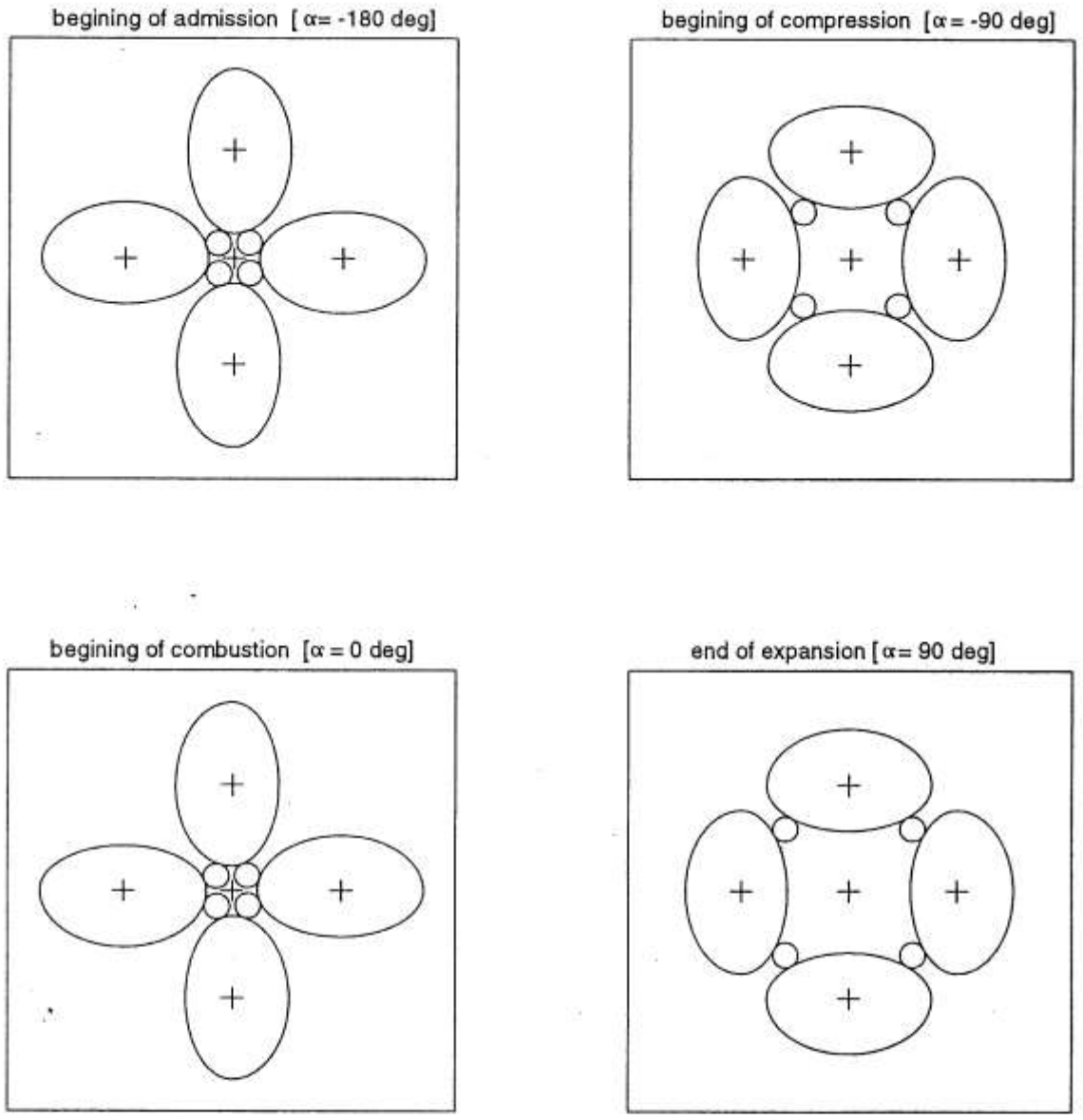

Figure 2 - Kinematics of the new mechanism: positon of the ellipses with respect to the angle of rotation α.

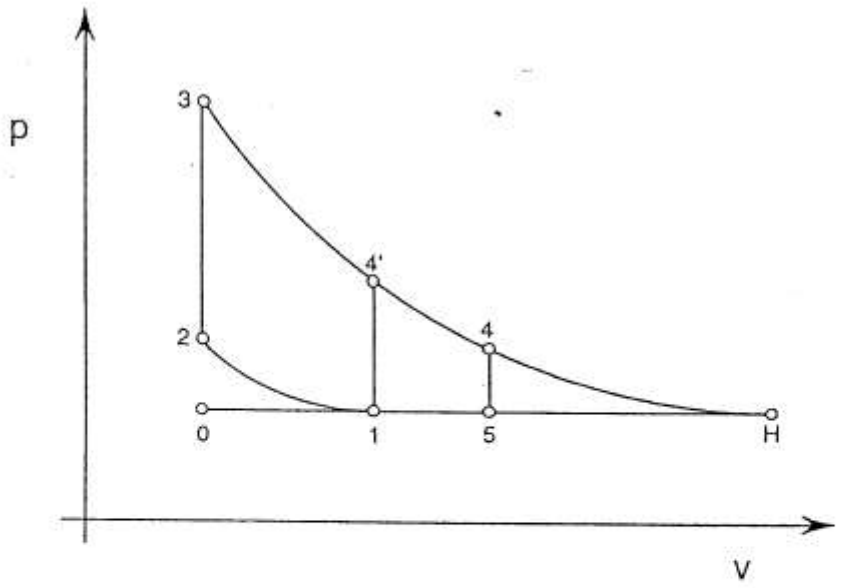

Figure 3 - Schematic diagram pressure x volume for the Otto cycle. The behaviour of the crank-piston and the cylindroids mechanisms. The maximum hypothetical volume to be achieved.

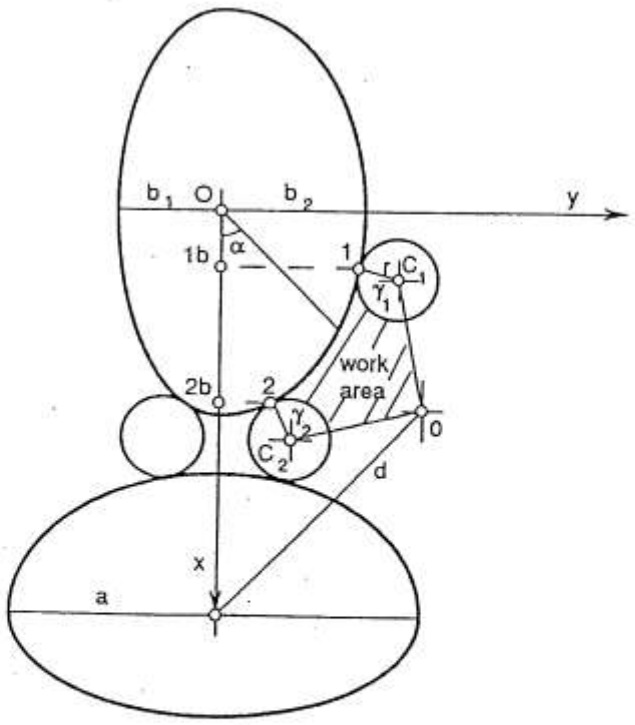

Figure 4 - The geometrical parameters. The work area. The local coordinates system.

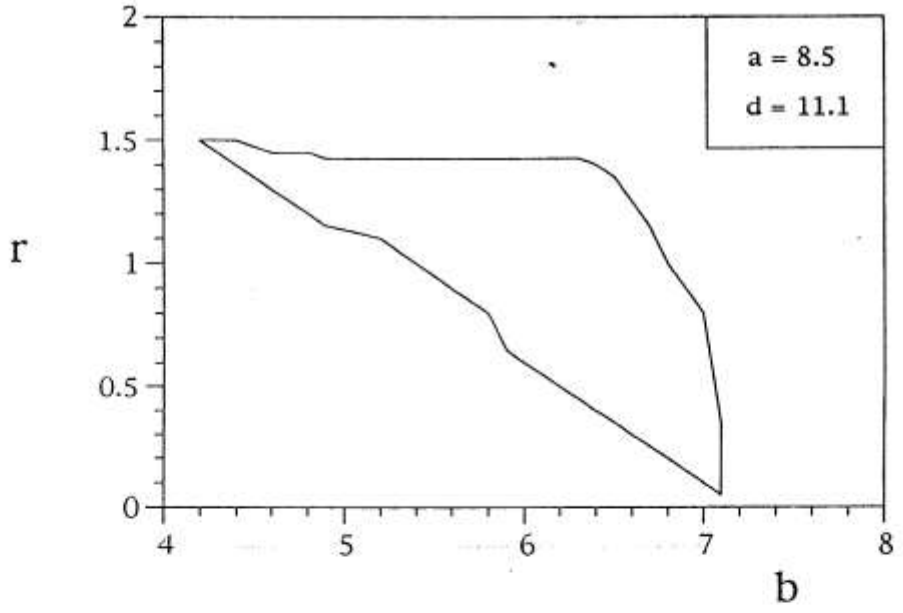

Figure 5 - Region (r,b) that satisfies the kinematics constraints.

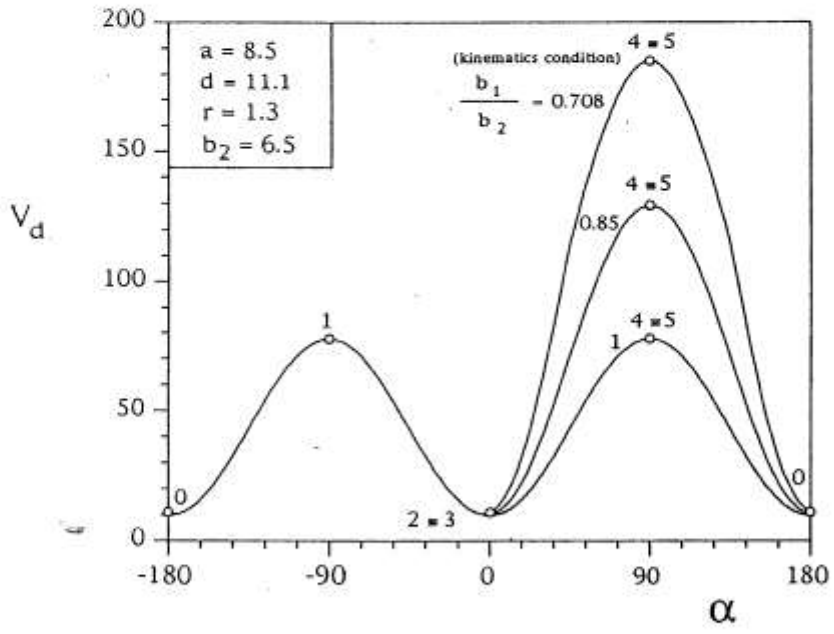

Figure 6 - The volume variation of the new mechanism, according to the angle position.

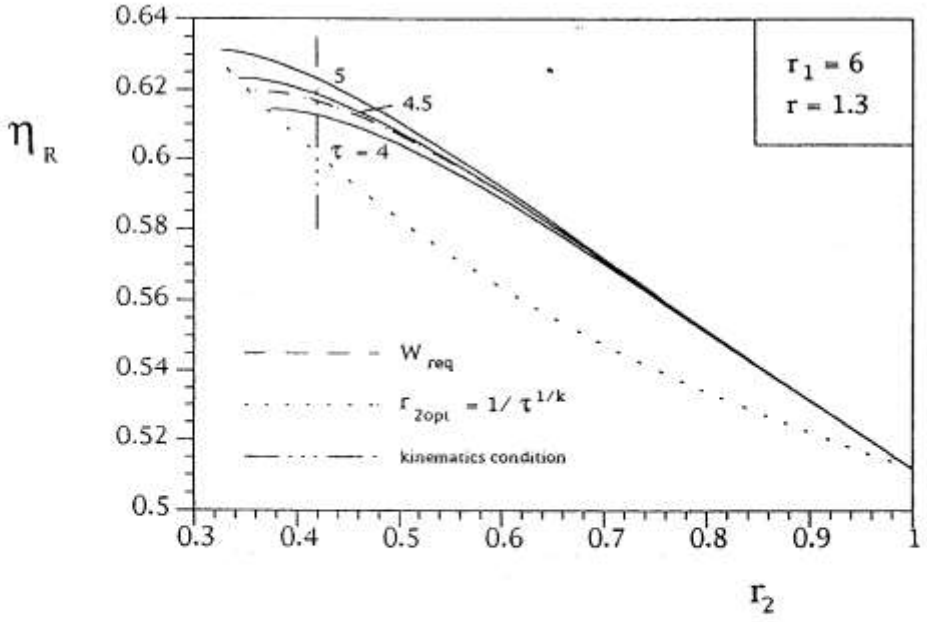

Figure 7 - Efficiency of the rotary engine for the air cycle.

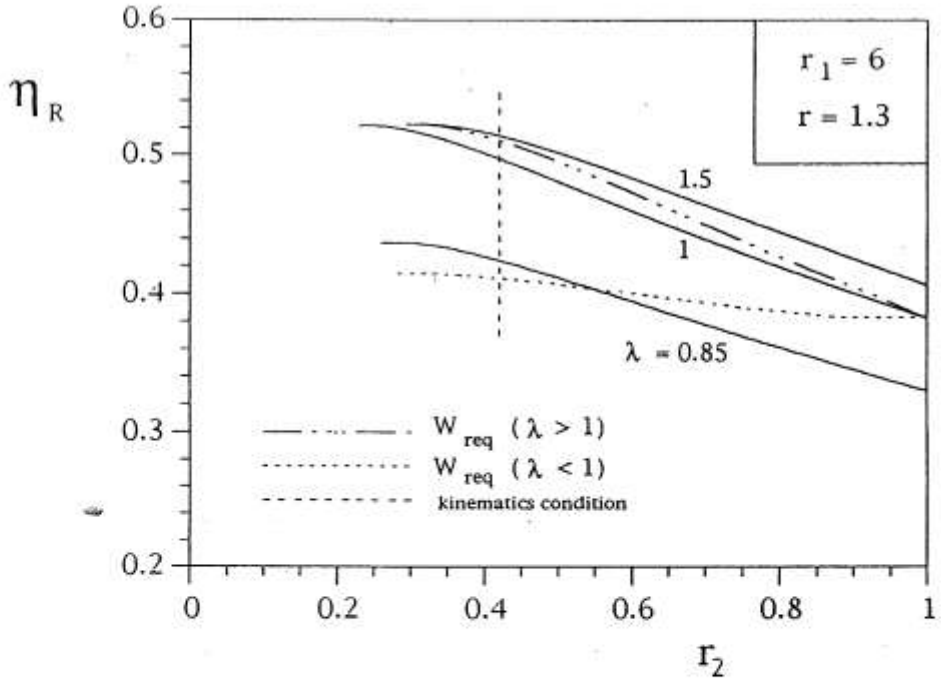

Figure 8 - Efficiency of the rotary engine for the fuel-air cycle.

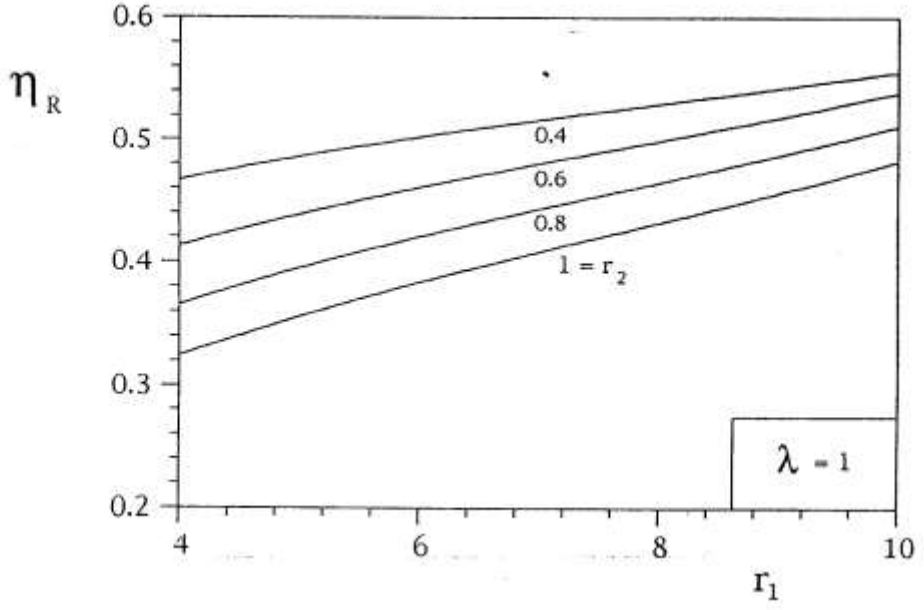

Figure 9 - Efficiency gain of the rotary engine, with respect to (r_1, r_2) for $\lambda = 1$.

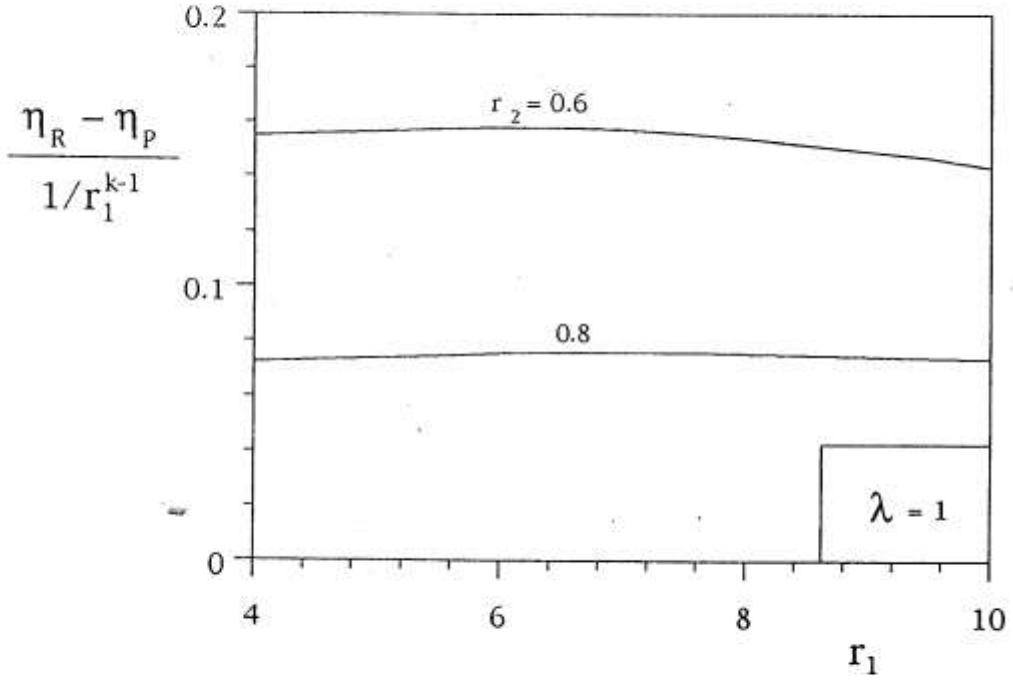

Figure 10 - Normalized efficiency difference as a function of r_1.

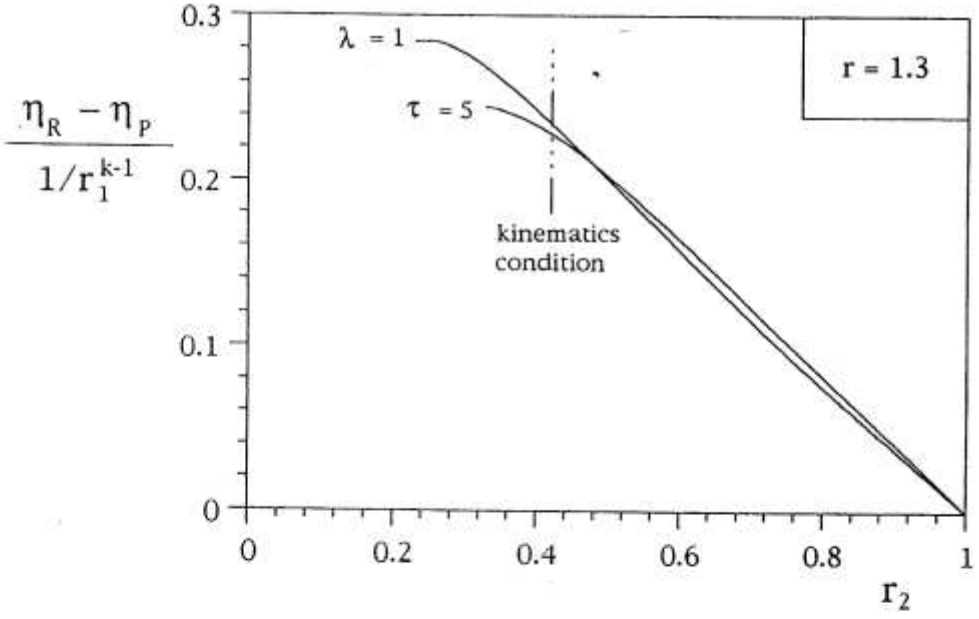

Figure 11 - Normalized efficiency difference as a function of r_2.

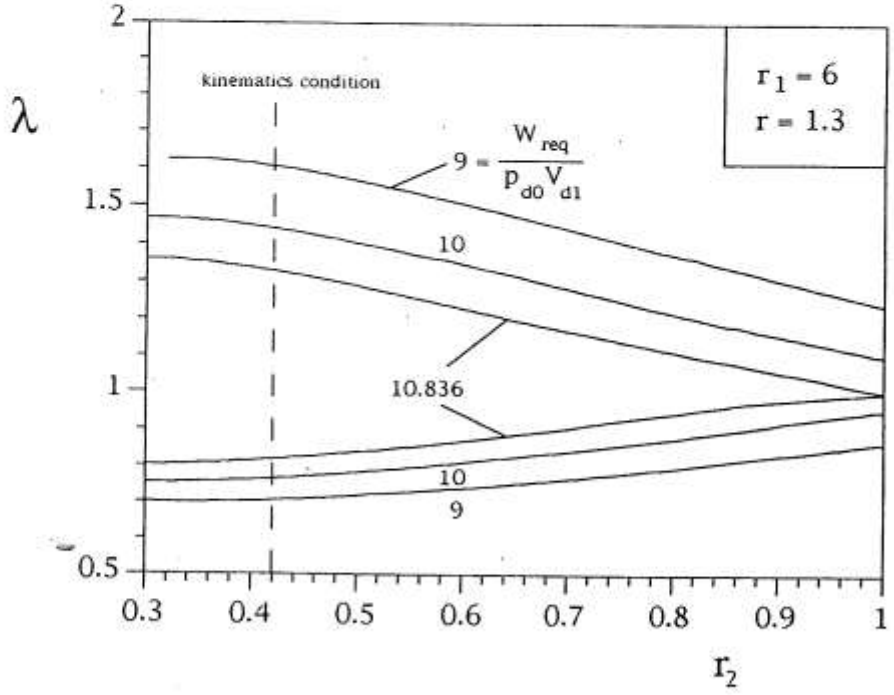

Figure 12 - Required work condition on the fuel-air cycle.